Antibody Delivery

DOI: 10.1002/anie.200905264

Efficient Delivery of Bioactive Antibodies into the Cytoplasm of Living Cells by Charge-Conversional Polyion Complex Micelles**

*Yan Lee, Takehiko Ishii, Hyun Jin Kim, Nobuhiro Nishiyama, Yoshiyuki Hayakawa, Keiji Itaka, and Kazunori Kataoka**

Antibodies are the most important component of humoral immunity, and can recognize and deactivate their corresponding extracellular antigens with outstanding selectivity. Moreover, the development of monoclonal and humanized antibodies has contributed greatly to the recent success of antibodies as biopharmaceuticals.[1] However, the target of such antibodies is limited to the cell exterior because of the lack of a delivery system of antibodies into the interior of the cell. Although the detection or inactivation of an intracellular protein was partially accomplished by the intracellular expression of antibodies,[2] the development of an efficient and safe delivery method of an antibody into living cells is required for further advances in therapeutics and bioanalysis. Various methods, such as microinjection, liposomes, cell-penetrating peptides, and even recombinant viruses, have been introduced;[3] however, their general use is often limited because of the need for highly specialized devices, as well as the complexity and inefficiency of these methods.

We recently developed a novel protein-delivery system into cytoplasm based on charge-conversional polyion complex (PIC) micelles.[4] The charge density of a model protein, cytochrome *c*, can be temporarily increased by the modification of the ε-amines of lysine residues into charge-conversional moieties, citraconic acid amide (Cit) or *cis*-aconitic acid amide (Aco) (Figure 1). As the positively charged lysines convert to the negatively charged carboxylic groups by this modification, the modified proteins become strongly anionic and the resulting charge density can be increased significantly to form stable PIC micelles with cationic block copolymers even at physiological salt concentrations. The charge-converted proteins and the cationic block in the copolymer form the core of the PIC micelle, and the polyethylene glycol (PEG) block forms the surface shell. After the PIC micelles were internalized to cells, the Cit and Aco rapidly degraded to reproduce the original lysines at the endosomal pH of 5.5.[5] The dissociation of the PIC micelles follows the regeneration of the original protein to release the free cationic block copolymer, which induces the pH-dependent destabilization

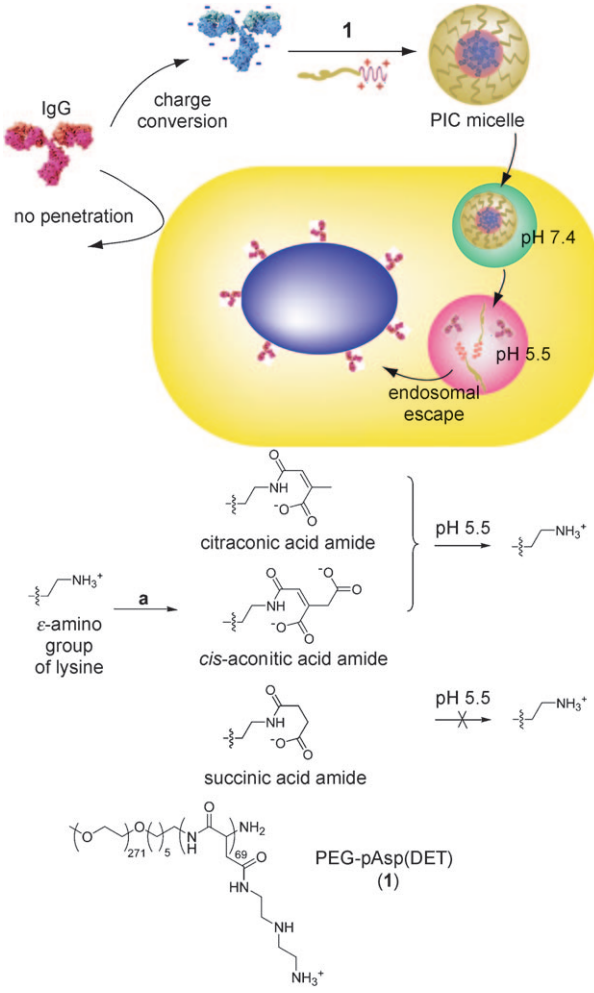

Figure 1. Preparation of the charge-conversional PIC micelles between IgG derivatives and PEG-pAsp(DET). a) Citraconic anhydride, *cis*-aconitic anhydride, or succinic anhydride. IgG = immunoglobulin G, PEG-pAsp(DET) = PEG-poly{*N*-[*N*′-(2-aminoethyl)-2-aminoethyl]aspartamide}.

[*] Dr. T. Ishii, Prof. Dr. K. Kataoka
Department of Bioengineering, The University of Tokyo
7-3-1 Hongo, Bunkyo-ku, Tokyo 113-8656 (Japan)
Fax: (+81) 3-5841-7139
E-mail: kataoka@bmw.t.u-tokyo.ac.jp
Dr. Y. Lee
Department of Chemistry, Seoul National University
Sillim-dong, Gwanak-gu, Seoul 151-742 (Korea)
H. J. Kim, Y. Hayakawa, Prof. Dr. K. Kataoka
Department of Materials Engineering
The University of Tokyo (Japan)
Dr. N. Nishiyama, Dr. K. Itaka, Prof. Dr. K. Kataoka
Center for Disease Biology and Integrative Medicine
Graduate School of Medicine, The University of Tokyo (Japan)
Dr. N. Nishiyama, Dr. K. Itaka, Prof. Dr. K. Kataoka
Center for Nanobio Integration, The University of Tokyo (Japan)

[**] This work was supported by a Core Research for Evolutional Science and Technology (CREST) grant from the Japan Science and Technology Agency (JST).

Supporting information for this article is available on the WWW under http://dx.doi.org/10.1002/anie.200905264.

of the endosomal membrane to aid the endosomal escape of the protein into cytoplasm.[6]

In the present study, we applied the same concept to intracellular antibody delivery for the purpose of controlling a cell pathway. As the molecular weight of the PIC micelle is well over several megadaltons,[7] we expected that the charge-conversional PIC micelle could easily deliver full immunoglobulin G (IgG) molecules with a molecular weight of 150 kD, which are difficult to deliver into the cytoplasm of living cells.

First, we examined the change in bioselectivity after the charge-conversional modification of IgG by using fixed and permeated cells in which the plasma membrane is no longer a penetration barrier of antibodies. All experimental procedures are described in detail in the Supporting Information. The nuclear pore complex (NPC), which is a protein complex that controls the transport of biomolecules across the nuclear envelope, was selected as a target for the antibodies.[8] Although anti-NPC mouse IgG can recognize the NPC of fixed cells selectively (Supporting Information, Figure S1a), anti-NPC IgG modified with Cit (anti-NPC IgG-Cit) loses this selectivity (Supporting Information, Figure S1b). However, the selectivity of anti-NPC IgG-Cit is mostly recovered after incubation at pH 5.5 (Figure 2b), contrary to the result after incubation at pH 7.4 (Figure 2a). The rapid degradation of Cit at pH 5.5 allowed regeneration of the selectivity of anti-NPC IgG. The selectivity change of the other derivatives, anti-NPC IgG modified with Aco (anti-NPC IgG-Aco) and anti-NPC IgG modified with a nondegradable succinic acid amide (anti-NPC IgG-Suc), is shown in Figure S1 in the Supporting Information. As expected, nondegradable anti-NPC IgG-Suc showed no selectivity after incubation at either pH 7.4 or pH 5.5.

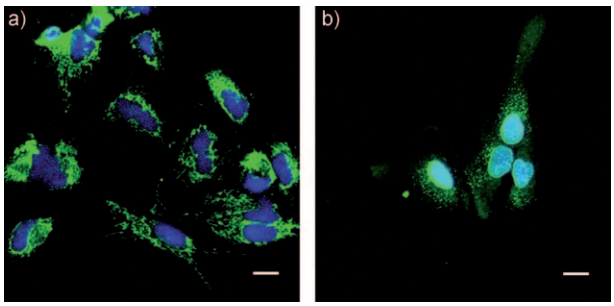

Figure 2. Recognition of NPC in fixed human hepatoma (HuH-7) cells by anti-NPC IgG-Cit after 4 h of incubation at a) pH 7.4 and b) pH 5.5. Anti-NPC IgG-Cit was applied to the cells after fixation. The cell nuclei were stained by Hoechst 33258 (blue), and the anti-NPC IgG-Cit was detected by a secondary antibody, the Alexa Fluor 488-labeled $(Fab')_2$ fragment from goat anti-mouse IgG (green). Scale bars: 20 μm. Fab = fragment, antigen-binding.

For the formation of PIC micelles, we selected PEG-poly{*N*-[*N*′-(2-aminoethyl)-2-aminoethyl]aspartamide} (PEG-pAsp(DET); **1**) as a cationic block copolymer. Compound **1** shows efficient cytoplasmic delivery of DNA and proteins with minimal cytotoxicity,[9] and thus we expected that the PIC micelles based on **1** would also be able to deliver IgG into cytoplasm efficiently. The formation of PIC micelles between the modified anti-NPC IgG derivatives and **1** was examined by dynamic light scattering (DLS; Table 1).

Table 1: Formation of PIC micelles containing IgG derivatives.

IgG derivative	Diameter [nm][a]	PDI[a,b]
anti-NPC IgG	N.D.[c]	N.D.
anti-NPC IgG-Cit	98.3	0.096
anti-NPC IgG-Aco	107	0.016
anti-NPC IgG-Suc	111	0.121

[a] Determined by DLS. [b] Polydispersity index. [c] Not determined.

Although the native anti-NPC IgG could not form the PIC micelles with **1**, anti-NPC IgG derivatives with increased charge densities were able to form PIC micelles successfully, even at physiological salt concentrations (150 mM NaCl). All PIC micelles showed unimodal size distributions (Supporting Information, Figure S2) with hydrodynamic diameters of around 100 nm.

The pH-dependent dissociation of the charge-conversional PIC micelles containing the antibody derivatives was confirmed by the fluorescence quenching/dequenching method.[10] Herein, we used Alexa Fluor 488-labeled IgG $(Fab')_2$ fragments from goat anti-mouse IgG as a payload in the PIC micelles instead of whole IgG molecules to chase the green fluorescence. The fluorescence intensity of the IgG $(Fab')_2$ derivatives in the core of the PIC micelles was reduced significantly as a result of the probe–probe quenching effect (20–30%). The decreased fluorescence intensity could be recovered after the release of the IgG $(Fab')_2$ from the PIC micelles (Supporting Information, Figure S4). Although the PIC micelles containing IgG $(Fab')_2$-Cit or IgG $(Fab')_2$-Aco were stable at pH 7.4, they dissociated rapidly at pH 5.5. The decrease of the charge density in IgG $(Fab')_2$ derivatives resulting from the pH-sensitive degradation of Cit and Aco is likely to be the main reason for this destabilization.

Next, we examined the intracellular trafficking of the charge-conversional antibodies on the living cells without fixation or permeation. Because the encapsulated IgG $(Fab')_2$ derivatives were labeled with Alexa Fluor 488 (green) and the late endosomes and lysosomes were stained with Lysotracker Red (red), the IgG $(Fab')_2$ in the endosome showed yellow fluorescence as a result of the co-localization of green and red fluorescence. The IgG $(Fab')_2$ was detected as green only after endosomal escape. IgG $(Fab')_2$-Cit showed efficient endosomal escape (Figure 3a), whereas IgG $(Fab')_2$-Aco and IgG $(Fab')_2$-Suc showed limited endosomal escape (Figure 3b,c). The degrees of endosomal escape are summarized in Figure 3d as a co-localization ratio between the green and red fluorescence; the lower the co-localization ratio, the more efficient the endosomal escape. The most efficient endosomal escape of the Cit derivative corresponds to our previous result.[4b] Because pH-sensitive protonation and direct contact with the endosomal membrane of the pAsp(DET) block are essential for endosomal destabilization,[11] the lowest endosomal escape of the nondissociable IgG $(Fab')_2$-Suc PIC micelle is reasonable.

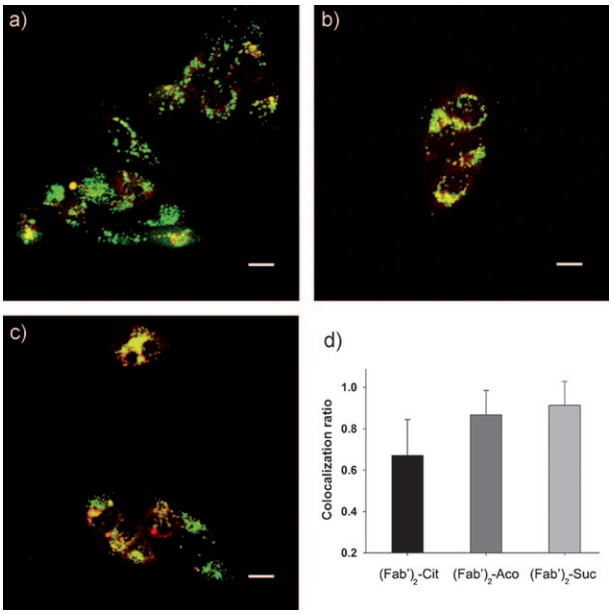

Figure 3. Confocal laser scanning microscopy (CLSM) images of HuH-7 cells treated with PIC micelles containing Alexa Fluor 488-labeled IgG $(Fab')_2$ fragment derivatives (green). a) $(Fab')_2$-Cit, b) $(Fab')_2$-Aco, and c) $(Fab')_2$-Suc. The late endosomes and lysosomes were stained with LysoTracker Red. Scale bars: 20 μm. d) Colocalization of the green fluorescence of $(Fab')_2$ derivatives and the red fluorescence of Lysotracker Red. Error bars: standard deviation.

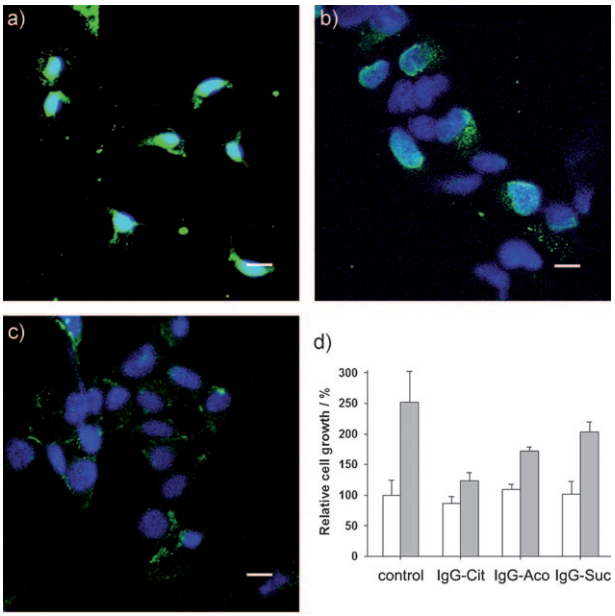

Figure 4. CLSM images of HuH-7 cells treated with PIC micelles containing a) anti-NPC IgG-Cit, b) anti-NPC IgG-Aco, and c) anti-NPC IgG-Suc. The cell nuclei were stained by Hoechst 33258 (blue), and the IgG derivatives were detected by a secondary antibody, the Alexa Fluor 488-labeled $(Fab')_2$ fragment from goat anti-mouse IgG (green). Scale bars: 20 μm. d) Growth of HuH-7 cells treated by each type of PIC micelle. White and gray bars represent the relative cell growth after 24 and 48 h of incubation, respectively. Error bars: standard deviation.

Finally, we examined the recognition of the NPC by the intracellular delivery of anti-NPC IgG into living cells by PIC micelles. The intracellular distribution of anti-NPC IgG released from the micelles was visualized by treating the cells with a secondary antibody, the Alexa Fluor 488-labeled $(Fab')_2$ fragment from goat anti-mouse IgG (green), after fixation. Note that the IgG derivative segregated in the core of PIC micelles may not be detected by this procedure; however, the released IgG can be selectively visualized in the cell. Anti-NPC IgG-Cit showed excellent recognition activity of NPC compared to the other IgG derivatives. The strong aquamarine fluorescence from the co-localization of the anti-NPC IgG (green) and the nucleus (blue) clearly represents NPC recognition by the anti-NPC IgG released from the anti-NPC IgG-Cit PIC micelles (Figure 4a). Anti-NPC IgG-Aco also recognized the NPC, but the intensity of its green fluorescence was lower than that of anti-NPC IgG-Cit, probably because of its limited endosomal escape efficiency (Figure 4b). The non-charge-conversional control, anti-NPC IgG-Suc, showed no selectivity on the nuclear envelope (Figure 4c).

The control of cell growth by the delivery of charge-conversional intracellular antibodies was confirmed by counting cell numbers (Figure 4d). As NPC controls the transport of essential biomolecules between the nucleoplasm and cytoplasm, the recognition and deactivation of NPC by anti-NPC IgG are critical for cell growth. Cells that were treated with anti-NPC IgG-Suc PIC micelles showed almost no change in cell growth, whereas those treated with anti-NPC IgG-Cit micelles showed a significant reduction in cell growth ($P < 0.05$) after 48 h. The effect of the anti-NPC IgG-Aco PIC micelles was midway between those of anti-NPC IgG-Cit and anti-NPC IgG-Suc. A comparison with control data from a nonspecific IgG (IgG1 kappa) is shown in Figure S6 in the Supporting Information.

In summary, we have successfully delivered biologically active IgG into cytoplasm by the charge-conversional PIC micelle method for controlling cell growth. Considering that an antibody has outstanding selectivity on its corresponding antigen, the concept of charge-conversional intracellular antibody delivery reported here is expected to have high potential for the bioimaging of the intracellular structures and functions of living cells, as well as for biotherapeutics to target intracellular antigens. Moreover, charge-conversional PIC micelles could be used in intravenous protein delivery, based on the high biocompatibility and elongated circulation provided by the PEG shell of the PIC micelles. New therapeutic strategies with both specificity and efficiency may also be expected through the combination of an antibody-based ligand for the recognition of a specific extracellular antigen on the cell surface and the charge-conversional antibody for the deactivation of an intracellular antigen.

Received: September 21, 2009
Published online: March 5, 2010

Keywords: antibodies · biological activity · charge conversion · drug delivery · micelles

[1] a) G. Köhler, C. Milstein, *Nature* **1975**, *256*, 495 – 497; b) M. J. Glennie, J. G. J. van de Winckel, *Drug Discovery Today* **2003**, *8*, 503 – 510; c) R. A. Lerner, *Angew. Chem.* **2006**, *118*, 8284 – 8305; *Angew. Chem. Int. Ed.* **2006**, *45*, 8106 – 8125.
[2] M. Stocks, *Curr. Opin. Chem. Biol.* **2005**, *9*, 359 – 365.
[3] a) K. H. Antman, D. M. Livingston, *Cell* **1980**, *19*, 627 – 635; b) C. A. Lackey, O. W. Press, A. S. Hoffman, P. S. Stayton, *Bioconjugate Chem.* **2002**, *13*, 996 – 1001; c) M. C. Morris, J. Depollier, J. Mery, F. Heitz, G. Divita, *Nat. Biotechnol.* **2001**, *19*, 1173 – 1176; d) B. Cornelissen, M. Hu, K. McLarty, R. M. Reilly, *Nucl. Med. Biol.* **2007**, *34*, 37 – 46; e) Y. Kondo, K. Fushikida, T. Fujieda, K. Sakai, K. Miyata, F. Kato, M. Kato, *J. Immunol. Methods* **2008**, *332*, 10 – 17.
[4] a) Y. Lee, S. Fukushima, Y. Bae, S. Hiki, T. Ishii, K. Kataoka, *J. Am. Chem. Soc.* **2007**, *129*, 5362 – 5363; b) Y. Lee, T. Ishii, H. Cabral, H. J. Kim, J. H. Seo, N. Nishiyama, H. Oshima, K. Osada, K. Kataoka, *Angew. Chem.* **2009**, *121*, 5413 – 5416; *Angew. Chem. Int. Ed.* **2009**, *48*, 5309 – 5312.
[5] a) J. K. Shetty, J. E. Kinsella, *Biochem. J.* **1980**, *191*, 269 – 272; b) Y. Lee, K. Miyata, M. Oba, T. Ishii, S. Fukushima, M. Han, H. Koyama, N. Nishiyama, K. Kataoka, *Angew. Chem.* **2008**, *120*, 5241 – 5244; *Angew. Chem. Int. Ed.* **2008**, *47*, 5163 – 5166.
[6] K. Miyata, M. Oba, M. Nakanishi, S. Fukushima, Y. Yamasaki, H. Koyama, N. Nishiyama, K. Kataoka, *J. Am. Chem. Soc.* **2008**, *130*, 16287 – 16294.
[7] A. Harada, K. Kataoka, *Macromolecules* **1998**, *31*, 288 – 294.
[8] K. J. Ryan, S. R. Wente, *Curr. Opin. Cell Biol.* **2000**, *12*, 361 – 371.
[9] a) N. Kanayama, S. Fukushima, N. Nishiyama, K. Itaka, W.-D. Jang, K. Miyata, Y. Yamasaki, U.-I. Chung, K. Kataoka, *ChemMedChem* **2006**, *1*, 439 – 444; b) K. Masago, K. Itaka, N. Nishiyama, U. Chung, K. Kataoka, *Biomaterials* **2007**, *28*, 5169 – 5175.
[10] a) B. Z. Packard, A. Komoriya, D. D. Toptygin, L. Brand, *J. Phys. Chem. B* **1997**, *101*, 5070 – 5074; b) Y. Lee, H. Mo, H. Koo, J.-Y. Park, M. Y. Cho, G. Jin, J.-S. Park, *Bioconjugate Chem.* **2007**, *18*, 13 – 18.
[11] S. Takae, K. Miyata, M. Oba, T. Ishii, N. Nishiyama, K. Itaka, Y. Yamasaki, H. Koyama, K. Kataoka, *J. Am. Chem. Soc.* **2008**, *130*, 6001 – 6009.

